RSC Advances

ROYAL SOCIETY OF CHEMISTRY

www.rsc.org/advances

Investigation on Micelle Formation by *N*-(Diethyleneglycol) Perfluorooctane Amide Fluorocarbon Surfactant as a Foaming Agent in Aqueous Solution

Qing You[1,2], Zhuojing Li[1,2], Qinfang Ding[3], Yifei Liu[3], Mingwei Zhao[3], Caili Dai[3]

1. School of Energy Resources, China University of Geosciences (Beijing)
2. Key Laboratory of Marine Reservoir Evolution and Hydrocarbon Accumulation Mechanism, Ministry of Education, China University of Geosciences (Beijing)
3. School of Petroleum Engineering, China University of Petroleum (East China)

---

*Corresponding author. Tel.: +86-13911326678.

E-mail address: youqing@cugb.edu.cn

ABSTRACT: Micelles formed by nonionic fluorocarbon surfactant *N*-(diethyleneglycol) perfluorooctane amide as a foaming agent due to its excellent foaming performance in aqueous solution were studied through surface tension, dynamic light scattering, isothermal titration calorimetry, and dissipative particle dynamic simulation. The surface activity, adsorption, and thermodynamic parameters (ΔG_m^0, ΔG_{ads}^0, ΔH_m^0, ΔS_m^0, ΔH_m^A, $\Delta C_{p,m}^0$) of micellization were systematically investigated. The experimental results showed that this nonionic fluorocarbon surfactant had superior surface activity and the micelle formation was entropy-driven. The micelle formation was also demonstrated by dynamic light scattering and isothermal titration calorimetry. Furthermore, to better understand the micelle formation, dissipative particle dynamic (DPD) simulation was conducted to simulate the whole formation process.

Keywords: Nonionic fluorocarbon surfactant, Surface activity, Micelle formation, Thermodynamic parameters, Dissipative particle dynamic simulation

1. Introduction

Coalbed methane (CBM) as an important unconventional gas resource and strategic reserve resource has attracted much attention around the world[1]. The production of CBM is generally conducted using hydraulic fracturing as an effective technique[2]. In general, the hydraulic fracturing fluids can be sorted into many kinds, such as clean water, guar gum, cross-linking gel, viscoelastic surfactant and foam. Among them, foam fracturing fluid has been widely used in CBM reservoir and other unconventional reservoirs because of its good sand-carrying capacity, easy flow-back, less usage and low damage to the formations in the recent years[3-5]. The effect of fracturing process is dependent on the properties, especially the foaming property of foam fracturing fluid. Based on this, the foaming agent decides the properties of fracturing fluids and thus is the key research emphasis.

The foaming agent is generally selected from surfactants with high surface activity, such as sodium dodecyl sulfate, dodecyl sulphate, lauroyl diethanolamide. Rajendra and Bhagwat studied the foaming properties of three surfactants, including sodium laureth sulfate (SLS), Triton X-100 and Brij 58[6]. Pugh group investigated the surface tension and foamability of a series of polypropylene glycols (PPG) surfactants. The results showed that the molecular weight of PPG have significant effect on the foamability of PPG foamers. Li and Yi studied the CO_2 foam flood project using quarternary ammonium salt surfactant as the foaming agent. The results showed good application performance of flood system [7]. Although there have been many reports about the foaming agents, how to produce CBM more effectively is still a challenge, especially the selection of effective foaming agents.

As is known, the foamability of surfactant is closely related to the surface activity and self-assembled aggregates in aqueous solution. Self-assembled aggregates, including micelles, vesicles, lyotropic crystals, and microemulsions, have attracted a large amount of attention due to their wide applications in cosmetics, drug delivery, nanomaterials synthesis and enhanced oil recovery[8-10]. The investigation of these self-assembled aggregates has been of fundamental interest over these past 20 or 30 years. The most common self-assembled aggregates are micelles formed by various surfactants in aqueous solution with the surfactant concentration larger than cmc. Among so many different kinds of surfactants, fluorocarbon surfactants have attracted much attention due to their super surface activity and rich phase behaviors in the recent years. Micelle formation by fluorocarbon surfactant in aqueous solutions has

been a classical field of investigation in surfactant sciences since Klevens and Shinoda[11-14]. Fung and Mamrosh synthesized a new kind of nonionic fluorocarbon surfactant ($C_nF_{2n+1}C(O)NH(CH_2CH_2O)_mH$; n=3, 6-8; m=2-4), which showed a series of unusual micellar characteristics in aqueous solution[15]. Eastoe research group synthesized another nonionic fluorocarbon surfactant ($X(CF_2)_mCH_2O(C_2H_4O)_3CH_3$; X=H or F; m=4 or 6). The results indicated the relationship between structure and surface activity, and relationship between terminal groups and its properties[16]. Rekha Goswami Shrestha and Lok Kumar Shrestha studied self-assembled structures of the nonionic fluorocarbon surfactant ($C_8F_{17}SO_2N(C_3H_7)(CH_2CH_2O)_{20}H$), and indicated that the spherical micelles can grow into cylindrical micelles, which entangle to form a rigid network structure of wormlike micelles above a certain concentration[17]. Our group also studied the micellar behaviors of a synthesized nonionic fluorocarbon surfactant ($(C_7F_{15})CONHC_2H_3(OH)CH_3$)[8]. A series of adsorption parameters at the air-water interface showed the superior surface activity of the above nonionic fluorocarbon surfactant. This super surface activity makes fluorocarbon surfactants have potential to be the foaming agents. For the components of foam fracturing fluids for producing CBM, the nonionic fluorocarbon surfactants are preferred to decrease the adsorption amount of surfactant on coal surface, due to the negative charges and complex headgroups of coalbed surface.

In this work, a series of nonionic fluorocarbon surfactants are synthesized. The *N*-(diethyleneglycol) perfluorooctane amide (NPFOA) is selected as a foaming agent due to its excellent foaming performance. To the best of our known, this may be the first time to study the fluorocarbon surfactants used as the foaming agent. In general, the fluorocarbon surfactants are used in proton transporting materials for polymer electrolyte membrane fuel cells, oxygen-transporting gels for surgery, and drug-delivery systems. The surface activity, adsorption, and thermodynamic parameters of micellization for NPFOA are systematically investigated. Furthermore, the dissipative particle dynamic (DPD) simulation is also conducted to study the process of micelle formation. Through this work, we expect to gain much more understanding of the phase behaviors of fluorocarbon surfactant and broaden its application area.

2. Experimental section

2.1 Chemicals

A series of nonionic fluorocarbon surfactants were synthesized according to the reference reported[19,20]. Under the protection of nitrogen atmosphere, 16.235 g perfluorocaprylicacid, 3.765 g methanol, and 0.100 g acetic acid were added into a three-neck flask. The temperature was maintained at 40 °C and the mixture was stirred for 2 h. Then, 4.706 g monoisopropanolamine or (6.588 g diglycolamine, 8.435 g diisopropanolamine, 6.588 g diethanolamine) and 0.124 g (or 0.133 g, 0.142 g, 0.133 g) sodium methoxide were added to the flask and temperature was kept at 80 °C. After mixing for 4 h, the reaction was finished. The mixture was cooled and diluted with saturated saline solution, and extracted with ether. Then the ether extract was distilled, and a dark yellow product was obtained. The water used was deionized water. The product yield of the above four nonionic fluorocarbon surfactants are 64%, 71%, 66% and 63%, respectively.

2.2 Methods

(1) Foaming Performance

Ross foamer device was used to evaluate the foaming properties. Put 15 ml 0.2% foaming agent solution into the Foamer Device. Inject 150 ml nitrogen into the foamer device by dosing pump. Record foam volume as *V versus* time. Record the time when the foam volume drops to half of the original volume, which is called half-life period. The half-life period, marked as $t_{½}$, is used to evaluate the stable property. Measure three times of each sample and calculate the average value. The foam integrated value *F* is defined as the product of foam volume and half-life period, and calculate it according to the following equation, which is generally regarded as the measure of the foam ability of foaming agent.

$$F=V\times t_{½} \quad (1)$$

(2) Surface Tension

Surface tension measurement was carried out on a Model JYW-200B surface tensiometer (Chengde Dahua Instrument Co. Ltd., accuracy ±0.01 mN/m) using the ring method. Temperature was controlled by thermostat cell holder. The surface tension was determined by a single-measurement method and all measurements were repeated at least three times.

(3) Dynamic Light Scattering (DLS)

The DLS measurement was carried out to determine the hydrodynamic radius of micelles formed in aqueous solution using the Zetasizer Nano ZS (Malvern). The

DLS measurement was conducted at 25.0 ± 0.1 ℃. The scattering angle is 90° and the light wavelength is 632.8 nm from a solid-state He−Ne laser (22 mW) as the incident beam. Each sample of 1.5 mL solution was transferred to a square cuvette and DLS data were presented from the mean values of three measurements.

(4) Isothermal Titration Microcalorimetry (ITC)

The ITC was tested on a nanowatt-scale isothermal titration microcalorimeter (Thermometric 2277 Thermal Activity Monitor, Thermometric, Sweden). The 1 mL sample cell of the calorimeter was initially loaded with water. The surfactant solution (the titrant with a concentration of five times of cmc) was injected into the stirred sample cell using a 500-μL Hamilton syringe controlled by a Thermometric 612 Lund Pump. The interval between adjacent injections was 50 min, which was sufficiently long for the signal to return to the baseline. The golden turbine stirrer in the ampule was at a constant speed of 50 rpm throughout the experiment. All experiments were performed at 25.0 ^{o}C and repeated twice to achieve the reproducibility within ±2%.

3. Results and Discussion

3.1 Foaming Performance

Ross foamer device was used to determine the foaming performance of fluorocarbon surfactant, which is generally estimated through foam volume, half-life period and foam integrated value. The foam volume and half-life period indicate the volume and the stability of generated foams, respectively. The foam integrated value is the product of the foam volume and half-life period. The larger the foam integrated value, the better foaming performance of a foaming agent. Table 1 shows the foaming performance of four kinds of fluorocarbon surfactants at 25 ^{o}C. Through comparing the foaming volume, the half-life period and the foam integrated value, these foaming parameters of *N*-(diethyleneglycol) perfluorooctane amide (NPFOA) were the maximum, indicating that NPFOA is the most suitable to be the foaming agent. When comparing the foam integrated value with the typical conventional hydrocarbon anionic foaming agent sodium dodecyl sulfate (SDS), which is generally used as foaming agent and the foam integrated value was 73500 mL·s, NPFOA has better foaming performance than hydrocarbon surfactant, indicating good foaming ability.

Table 1. The foaming performance of four kinds of surfactants at 25^{o}C

No.	surfactant	foaming volume/mL	half-life period/s	foam integrated value/mL·s

1	N-(2-hydroxypropyl) perfluorooctane amide	190±1.5	176±2	33443±644
2	N-(diethylene glycol) perfluorooctane amide	230±1	470±2	108102±930
3	N, N-bis (2 - hydroxypropyl) perfluorooctane amide	220±2	226±1	49722±672
4	N, N-dihydroxyethyl perfluorooctane amide	200±1	200±3	40003±800
5	sodium dodecyl sulfate	210±1	350±1	73501±560

3.2 Surface Properties and Micellization

Surface tension measurement was carried out to investigate surface properties of NPFOA in aqueous solution. Figure 1 shows the surface tensions of solutions *versus* concentrations at 25 ^{o}C. For the dilute NPFOA solution, the surface tension value decreases sharply compared with that of pure water (72mN/m), indicating the adsorption of NPFOA molecules at the air-water interface. With the increase of NPFOA concentration, the value of surface tension gradually decreases. Until NPFOA concentration reaches a much higher value, the surface tension no longer decreases and almost remains constant. It is suggested that the adsorption of NPFOA molecules on the air-water interface reaches saturation. The concentration of breakpoint in the surface tension curve is traditionally assigned as the cmc. With the further increase of NPFOA concentration, the NPFOA molecules form micelles in aqueous solution. From Figure 1, the cmc value of NPFOA in aqueous solution at 25 ^{o}C is about 1.50 mM, which is similar to the result from ITC measurement (shown in the Supporting Information, SI). In general, the cmc values are the sign of surface activities of surfactants. The smaller cmc values indicate better surface activity. Comparing the cmc values of conventional hydrocarbon nonionic surfactants with the same carbon atoms and the other nonionic fluorocarbon surfactants with the same perfluorocarbon chain, the cmc values of $C_7F_{15}COONa$ and $C_7F_{15}CONHC_2H_3(OH)CH_3$ are 36 and 3.09 mM, respectively[8], the cmc value of NPFOA is lower, which means NPFOA has better surface activity.

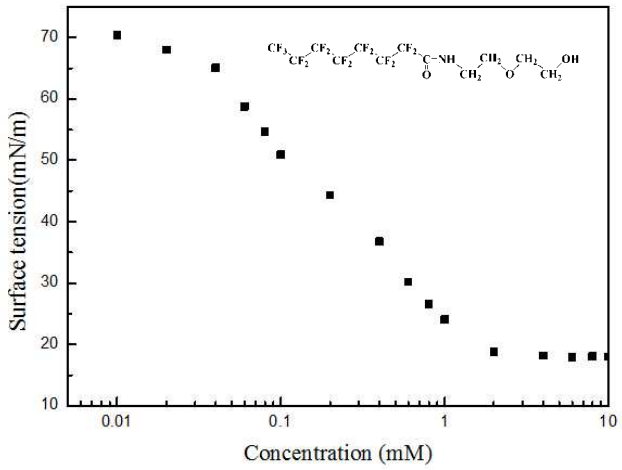

Figure 1. Surface tension *versus* concentration of NPFOA aqueous solution at 25 °C The inset image is the chemical formula of NPFOA.

For fluorocarbon surfactants, the most attractive characteristic is their ability to decrease the surface tension. From Figure 1, the lowest surface tension can reach 17.83 mN/m due to the adsorption of NPFOA at the air-water interface. In order to demonstrate the surface activity, the effectiveness of surface tension reduction (Π_{cmc}) is proposed and determined as follows:

$$\Pi_{cmc} = \gamma_0 - \gamma_{cmc} \qquad (2)$$

Wherein, γ_0 is surface tension of water; γ_{cmc} is surface tension of NPFOA aqueous solutions with the concentration exceeding cmc.

For NPFOA molecules, the Π_{cmc} can be calculated according to the equation (2), and the value is 54.17 mN/m. For the nonionic fluorocarbon surfactants with same perfluorocarbon chain, $C_8F_{17}SO_2N(C_3H_7)(C_2H_4)_{10}H$ (abbr. EF122B) and $C_8F_{17}SO_2N(C_3H_7)(C_2H_4)_{20}H$, have the remarkable ability to reduce surface tension with the Π_{cmc} values of 51.0 and 47.4 mN/m[19,21]. Through comparison, the NPFOA molecules have better ability to reduce surface tension. For the other types of fluorocarbon surfactants, such as anionic type $C_7F_{15}COONa$, and cationic type $C_3F_6O(C_3F_6O)_2C_2F_4CONH(CH_2)_3N^+(C_2H_5)_2CH_3I^-$ (abbr. FC-4), their minimum surface tensions of surfactant aqueous solutions are 24.2, and 18.4 mN/m[22]. Through comparison, the ability to reduce surface tension of NPFOA is better than

that of ionic fluorocarbon surfactants. Moreover, to further indicate the surface activity of NPFOA in aqueous solution, the relative maximum reduction of surface tension (Π_{cmc}/γ_0) is proposed and considered as a measure of surface activity of a surfactant in aqueous solution. In general, the relative maximum reduction of surface tension is larger, showing the surface activity of surfactant is better. For NPFOA, Π_{cmc}/γ_0 is about 0.75. For the nonionic fluorocarbon surfactant EF122B, Π_{cmc}/γ_0 is about 0.71[22], which also indicates the superior surface activity of NPFOA.

As mentioned above, the reduction of surface tension in Figure 1 is attributed to the adsorption of NPFOA at the air-water interface. So the adsorption behavior is investigated. To indicate the adsorption of NPFOA, two parameters are introduced, the maximum surface excess concentration Γ_{max} and the minimum area A_{min} occupied per surfactant molecule at the air-water interface, which can be calculated according to the following equations[23]:

$$\Gamma_{max} = -\frac{1}{nRT}\left(\frac{d\gamma}{d\ln c}\right)_T \quad (3)$$

Wherein, n is the number of solute species whose concentration at the interface changes with the change of surfactant concentration c; R is the gas constant; T is the absolute temperature; γ is the surface tension; and $d\gamma/d(\ln c)$ is the slope of surface tension γ *vs* $\ln c$ dependence when the concentration is close to cmc.

The value of n is taken as 1 for NPFOA in aqueous solution. Then A_{min} can be obtained from equation (4):

$$A_{min} = \frac{1}{N_A \Gamma_{max}}(\times 10^{23}) \quad (4)$$

Wherein, N_A is Avogadro number.

For the adsorption of NPFOA on the air-water interface at 25 °C, the values of Γ_{max} and A_{min} are 2.41 μmol/m^2 and 69.02 Å^2， respectively, as listed in Table 2. For clear comparison, the corresponding adsorption parameters are also listed in Table 2.

Table 2. Surface Properties of NPFOA and PPFOA[18] in Aqueous Solution(25℃)

surfactant	cmc(mmol/L)	γ_{cmc}(mN/m)	Π_{cmc}(mN/m)	Γ_{max}(μmol/L)	A_{min}(Å^2)	N
NPFOA	1.54±0.08	17.83±0.08	54.17±0.08	2.40±0.01	69.21±0.36	10

PPFOA	3.09	15.78	56.22	2.36	70.48	10

For the other typical fluorocarbon surfactants, the A_{min} values of PPFOA and EF122B are 70.48 and 70.00 Å^2. Through comparison, NPFOA molecules have a smaller A_{min}, which leads to a little larger Γ_{max}, indicating that NPFOA molecules pack more densely at the air-water interface. This relatively higher packing density at the interface may be due to the molecular characteristic and structure of NPFOA.

As is known, when NPFOA at the air-water interface reaches adsorption saturation, micelles are formed by NPFOA molecules in aqueous solution. The aggregation number (N) is usually proposed and the value of N can be calculated according to equation (5)[24]:

$$N = \frac{4\pi L^2}{A_{min}} \quad (5)$$

Wherein, A_{min} is the minimum area occupied per surfactant molecule on the air-water interface obtained from equation (3); L is the hydrophobic length of surfactant. For NPFOA, the L is about 7.5 Å according to the molecular structure simulation. This equation is based on a hypothesis: the micelles are generally regarded as spherical. For NPFOA molecules, the value of N is about 10, which is very close to the nonionic fluorocarbon surfactant PPFOA with aggregation number of 10. This may be due to the steric hindrance effect induced by the NPFOA molecular structure.

To further study the micelles formed by NPFOA, the DLS measurement was carried out to determine the hydrodynamic radius of micelles formed in aqueous solution. Figure 2 shows the DLS result at NPFOA concentration of about 5 mM (a little larger than its cmc). It can be seen that the scattering peak is very sharp, which indicates the micelles formation and the uniform radius of micelles. The average hydrodynamic radius is about 24.36 nm with the polydispersity of 0.944.

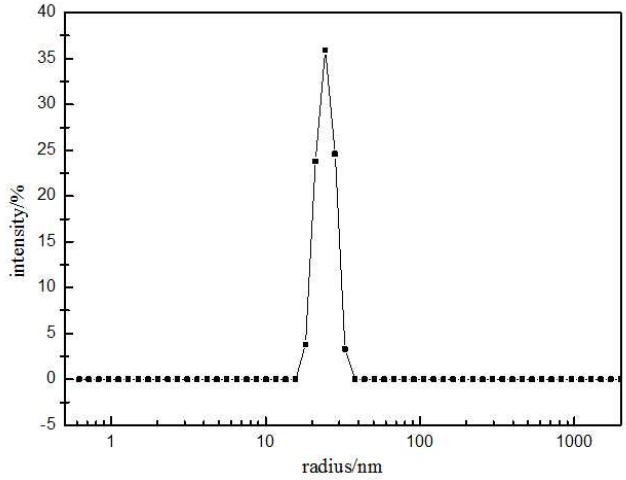

Figure 2. Size distribution of NPFOA micelles in aqueous solution (5mM, 25℃)

3.3 Thermodynamic Parameters of Micelle Formation

In general, temperature has a significant effect on the self-assembly behavior of surfactant in aqueous solution. Figure 3a shows the curve of surface tensions *versus* NPFOA concentrations at different temperatures. From Figure 3a, these curves show a similar tendency, and the ultimate surface tensions (γ_{cmc}) are almost the same. The cmc values at different temperatures can be easily obtained and are listed in Table 3. Figure 3b shows the relationship between temperature and the cmc values. It is clear that the cmc values increase with increasing temperature, and this plot fit a second-order polynomial, which can comply well with the other surfactants in aqueous solution[25-26].

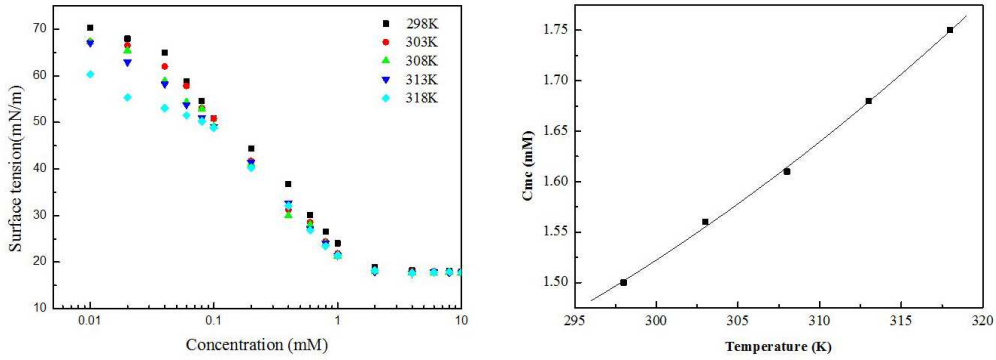

(3a) (3b)

Figure 3a. The curve of surface tensions versus NPFOA concentration. Figure 3b. The cmc values of NPFOA micelles at different temperature

Table 3. Thermodynamic parameters of NPFOA micelles formed in aqueous solution

surfactant	T(K)	cmc(mM)	ΔG_m^0(KJ/mol)	ΔH_m^0(KJ/mol)	$-T\Delta S_m^0$(KJ/mol)	ΔS_m^0(J/mol)
NPFOA	298	1.54±0.08	-26.00±0.168	-5.00±0.26	-21.06±0.092	70.67±0.309
	303	1.58±0.05	-26.37±0.150	-5.54±0.096	-20.83±0.054	68.75±0.178
	308	1.62±0.06	-26.74±0.158	-6.06±0.15	-20.68±0.008	67.14±0.026
	313	1.68±0.04	-27.08±0.146	-6.56±0.072	-20.52±0.074	65.56±0.236
	318	1.74±0.07	-27.42±0.165	-7.04±0.19	-20.38±0.025	64.09±0.079

For the thermodynamic parameters of micelles formed by NPFOA in aqueous solution, the standard Gibbs free energy of micelle formation (ΔG_m^0) can be calculated according to the pseudophase model of micellization from the equation below[27]:

$$\Delta G_m^0 = RT \ln X_{cmc} \qquad (6)$$

Wherein, R is the gas constant; T is absolute temperature; X_{cmc} is the cmc in molar fraction and can be transformed from cmc. By equation (6), the values of $\mathbf{\Delta} G_m^0$ at different temperatures can be obtained and are listed in Table 3. It is observed that the values of $\mathbf{\Delta} G_m^0$ increase negatively with the increase of temperature, which suggests that the formation of micelles becomes much more spontaneous. Furthermore, on the basis of the $\mathbf{\Delta} G_m^0$, the standard Gibbs free energy of adsorption ($\mathbf{\Delta} G_{ads}^0$) can also be calculated by equation (7)[24]. For NPFOA molecules, the value of ΔG_{ads}^0 at 25 °C is about -48.54 kJ/mol, which is similar to the nonionic fluorocarbon surfactants PPFOA reported with the ΔG_{ads}^0 value of -48.13 kJ/mol.

$$\mathbf{\Delta} G_{ads}^0 = \mathbf{\Delta} G_m^0 - \Pi_{cmc}/\Gamma_{max} \qquad (7)$$

Another thermodynamic parameter ΔH_m^0, the standard enthalpy of micellar formation can also be determined according to the following Gibbs-Helmholtz equation:

$$\Delta H_m^0 = [\frac{\partial(\Delta G_m^0/T)}{\partial(1/T)}] \qquad (8)$$

From the equation (8), the values of ($\Delta G_m^0/T$) are plotted as a function of ($1/T$), and the curve is shown in Figure 4a. The curve fits a second-order polynomial. The values of ΔH_m^0 at different temperatures are determined from slope of the tangential lines

and are listed in Table 3. Based on the results of ΔG_m^0 and ΔH_m^0, the standard entropy of micelle formation (ΔS_m^0) can be obtained by equation (9) and are listed in Table 3.

$$\Delta S_m^0 = (\Delta H_m^0 - \Delta G_m^0)/T \quad (9)$$

Figure 4b describes the relationship of thermodynamic parameters (ΔG_m^0, ΔH_m^0, and $-T\Delta S_m^0$) and temperature (T). The ΔH_m^0 and ($-T\Delta S_m^0$) represent the contributions of enthalpy change and enthalpy change to the standard Gibbs free energy of micelle formation, respectively. From the plots, with the increase of temperature, the variation of the Gibbs free energy is very slight, while the enthalpy variation decreases and the entropy variation increases remarkably. Comparing their contributions to ΔG_m^0, the entropy variation always plays a key role in the determination of ΔG_m^0. Thus, the micelle formation of NPFOA in aqueous solution is largely entropy-driven.

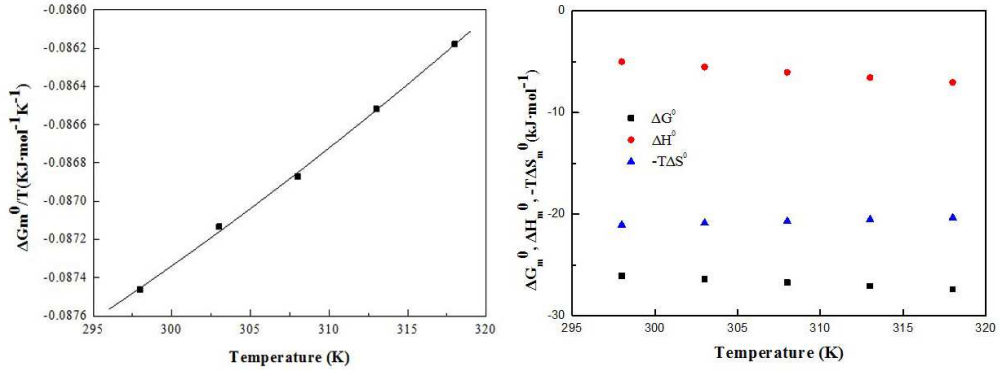

(4a) (4b)

Figure 4a. The plot of $\Delta G_m^0/T$ and T. Figure 4b. The plots of thermodynamic parameters (ΔG_m^0, ΔH_m^0, and ΔS_m^0) and T

For the variation of the enthalpy and entropy in aqueous solution, some linear relationship exists and it is usually called the entropy-enthalpy compensation[28-29]. It is meaningful to investigate the relationship between enthalpy and entropy variation for micelle formation of NPFOA in aqueous solution. The entropy-enthalpy compensation generally contains two parts: the desolvation part due to the dehydration of hydrophobic fluorocarbon chain and the chemical part due to the aggregation of surfactant tails to form micelles. Figure 5a shows the dependence of enthalpy change (ΔH_m^0) to entropy (ΔS_m^0). From this figure, the plot of ΔH_m^0 vs ΔS_m^0

shows a good linear relationship. The entropy-enthalpy compensation can be described in the following form:

$$\Delta H_m^0 = (\Delta H_m^A + T_c \Delta S_m^0) \quad (10)$$

Wherein, T_c is the compensation temperature and a measure of desolvation part; ΔH_m^A is the enthalpy belonging to the chemical part.

From the fitting of straight line, for NPFOA micelles formation, the values of ΔH_m^A and T_c are −26.73 kJ/mol and 307.4 K, respectively. This compensation temperature is similar to the nonionic fluorocarbon surfactant PPFOA reported before with ΔH_m^A and T_c values of -25.0 kJ/mol and 307.8 K[19]. The parameter ΔH_m^A represents the stability of micelles. The smaller the value ΔH_m^A, the more stable the micelles. Thus, compared with the nonionic fluorocarbon surfactants mentioned above, the NPFOA micelles are much more stable.

Another thermodynamic parameter $\Delta C_{p,m}^0$, the heat capacity of micellization was determined by the equation (11) below[30]:

$$\Delta C_{p,m}^0 = T(\partial \Delta S_m^0 / \partial T) \quad (11)$$

From the curve of micellization entropy as a function of temperature shown in Figure 5b, the plot fits a good linear relationship. The value of ΔC_{pm}^0 is about -0.33 kJ·mol^{-1}·K^{-1}, which is equal to the slope of fitting line, and a little bigger than the other nonionic fluorocarbon surfactant, such as PPFOA of -0.62 kJ·mol^{-1}·K^{-1}. The negative value of ΔC_{pm}^0 indicates that the hydration shell is lost in the process of micellization due to organized water molecules around the hydrophobic chain of surfactant. This discrepancy between NPFOA and PPFOA may be attributed to the changes in the aggregation numbers and shapes of the micelles.

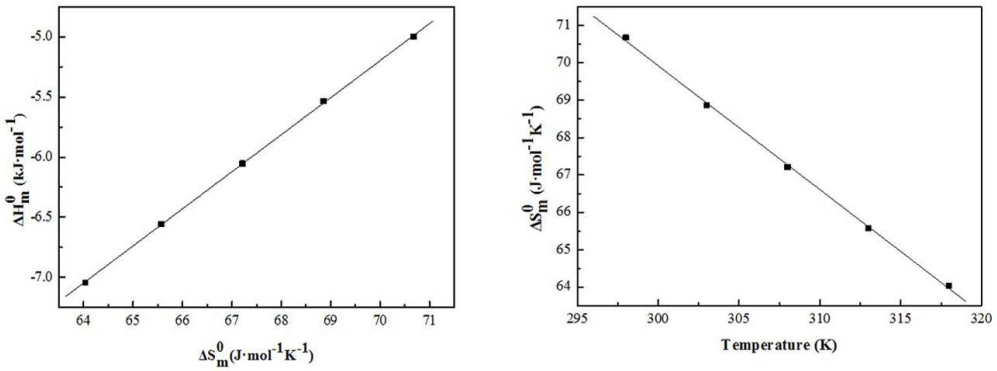

(5a) (5b)

Figure 5a. The relationship of enthalpy-entropy compensation. Figure 5b. ΔS_m^0 versus temperature for NPFOA in aqueous solution

3.4 Simulation Process of Micelle Formation

DPD simulations were carried out by Material Studio software. Detailed information for this simulation method can be obtained from previous reports [31-32]. In this simulation, the NPFOA molecule is represented by a dimeric model shown in Figure 6, where the amphiphilic molecule is divided into two parts, the hydrophilic part H and the hydrophobic part C, which are connected by a harmonic spring. The water molecule is represented by the monomer particle W. The interaction parameters aij between different particles are determined by using the blends model. They were as follows: $a_{C-C}=a_{H-H}=a_{W-W}$ =15, a_{C-H}=79.8, a_{C-W}=82.2, and a_{H-W}=0. The dynamics of 5000 DPD particles, starting from a random distribution, is simulated in a 10×10×10 cubic box under periodical boundary conditions. The step size for the integration of the Newton equation is set at Δt 0.05. The temperature is set at 298 K. In order to go into the dynamic process for micelle formation, DPD simulations were performed on the system with 20% NPFOA, and the corresponding results were shown in Figure 7. It can be seen that at the beginning stage, this system was not stable, and the beads in the system displayed an unordered arrangement (Figure 7a, 7b), indicating no ordered structure was formed. With time evolution, pre-micelles with spherical structure were formed accompanying some unordered structure, which can be clearly seen in Figure 7c. Then, they transformed to more ordered spherical micelles with time steps increased to 20000 (Figure 7d). Such an evolution process often occurs in tens of μs, and it is very difficult to observe directly by experimental methods. Therefore, the DPD simulated results are considered to be a great supplement for the experimental results, which can provide much more information of micro-phase separation.

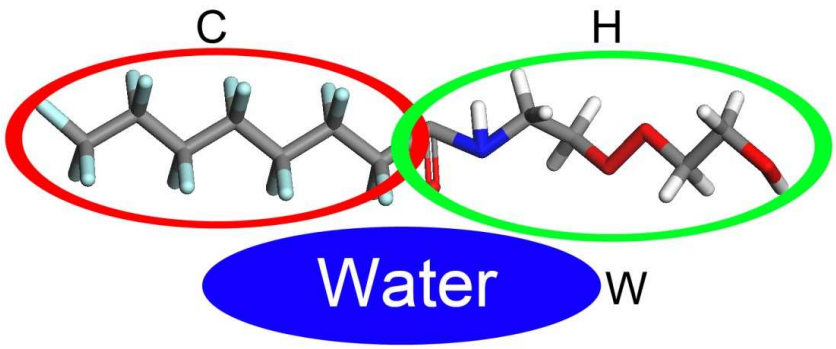

Figure 6. Schematic representation of the simulation model

The NPFOA molecule is divided into two DPD particles, fluorinated carbon chain (C) and headgroup (H), which are connected together by a harmonic spring. Water is represented by a single DPD particle W.

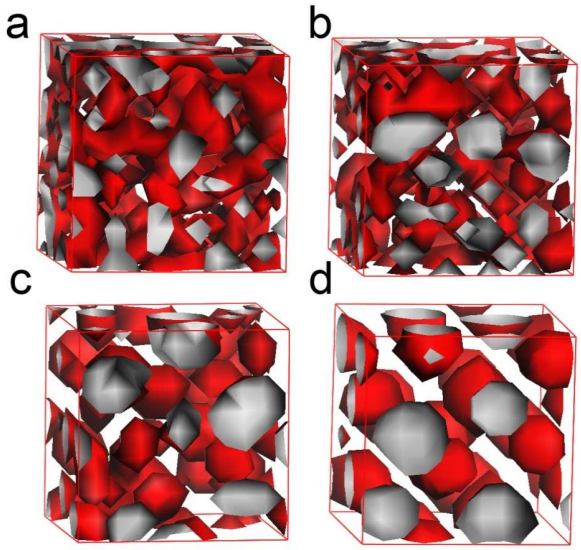

Figure 7. The simulated isodensity profiles for the micelles formed at room temperature at 20% NPFOA content at different time steps: (a) 3; (b) 10; (c) 100; and (d) 20000. The size of the simulation box is 10×10×10 in DPD units.

4. Conclusions

In summary, we investigated the micelle formation of the nonionic fluorocarbon surfactant NPFOA selected as a foaming agent due to best foaming performance in aqueous solution. NPFOA has a very low cmc value, showing good surface activity. The micelle formation is entropy-driven in the temperature range from 25 to 45^{o}C. The DPD further simulated the formation process of NPFOA micelles in aqueous

solution. Through this work, we expect to gain much more understanding of the phase behaviors of fluorocarbon surfactants and broaden its application area.

Acknowledgements

This work was supported by the Fundamental Research Funds for the Central Universities (No. 2-9-2014-007), Doctoral Fund from National Ministry of Education (No. 20120133110010) and the Joint Funds for CBM of Shanxi Province (No. 2013012003).

[1] T. A. Moore. Int. J. Coal Geol. 101 (2012) 36-81.

[2] Z. T. Li, F. X. Li, Z. W. Huang. Pet. Geol. Rec. Eff. 17 (2010) 76-81.

[3] M. W. Tan, X. G. He, S. B. Zhang. Drilling Prod. Technol. 31 (2008) 129-133.

[4] P. C. Harris. SPE Prod. Facilities 10 (1995) 197-203.

[5] Y. H. Ding, L. Z. Cong, Y. J. Lu. Pet. Explor. Development 29 (2002) 103-106.

[6] A. P. Powale, A. P. Andheria, S. S. Maghrabi, S. S. Bhagwat. J. Dispersion Sci. Technol. 26(2005)597-603.[7] C. Li, X. Y. Yi, W. Liu, Y. Lu. Oilfield Chem. 25(2007)255-257.

[8] E. Kissa. Marcel Dekker: New York (2001).

[9] C. Mille, R. W. Corkery. J. Mater. Chem. 1 (2013) 1849-1859.

[10] H. Kunieda, K. Nakamura, U. Olsson. J. Phys. Chem. 97 (1993) 9525-9531.

[11] H. B. Klevens. J. Phys. Chem. 54 (1950) 1012-1016.

[12] K. Shinoda, T. Soda. J. Phys. Chem. 67 (1963) 2072-2074.

[13] K. Shinoda, K. Katsura. J. Phys. Chem. 68 (1964) 1568-1569.

[14] K. Shinoda, T. Soda. J. Phys. Chem. 84 (1980) 365-369.

[15] B. M. Fung, D. L.Mamrosh, E. A. O'Rear. J. Phys. Chem. 92 (1988) 4405-4411.

[16] J. Eastoe, A. Paul, A. Rankin. Langmuir 17 (2001) 7873-7878.

[17] R. G. Shrestha, L. K. Shrestha, S. C. Sharma, K. Aramaki. J. Phys. Chem. B 112 (2008) 10520-10527.

[18] C. L. Dai, M. Y. Du, M. W. Zhao. J. Phys. Chem. B 117 (2013) 9922-9928.

[19] J. Hu. Shandong: China University of Petroleum (East China) (2009).

[20] Q. Cheng, X. M. Liu, C. L. Dai. Chin. J. Appl. Chem. 30(2011)1276-1280.

[21] S. C. Sharma, C. Rodríguez-Abreu, L. K. Shrestha, K. Aramaki. J. Colloid Interface Sci. 314 (2007) 223-229.[22] Y. A. Gao, W. G. Hou, Z. N. Wang, B. X. Han.

G. Y. Zhang. Chin. J. Chem. 23 (2005) 362-366.

[23] M. Blesic, E. Melo, Z. Petrovski, N. V. Plechkova, J. N. C. Lopes, K. R. Seddon, L. P. N. Rebelo. J. Phys. Chem. B 112 (2008) 8645-8650.

[24] M. N. Wadekar, J. Boekhoven, W. F. Jager, G. J. M. Koper, S. J. Picken. Langmuir 29 (2012) 3397-3402.

[25] M. W. Zhao, L. Q. Zheng. Phys. Chem. Chem. Phys. 13 (2011) 1332-1337.

[26] T. F. Tadros. J. Colloid Interface Sci. 74 (1980) 196-200.

[27] J. J. Wang, H. Y. Wang, S. L. Zhang, H. C. Zhang, Y. Zhao. J. Phys. Chem. B 111 (2007) 6181-6188.

[28] H. N. Singh, S. M. Saleem, R. P. Singh. J. Phys. Chem. 84 (1980) 2191-2194.

[29] Z. Bedo, E. Berecz, I. Lakatos. Colloid Polym. Sci. 270 (1992) 799-805.

[30] A. González-Pérez, J. M. Ruso, M. J. Romero, E. Blanco, G. Prieto, F. Sarmiento. Chem. Phys. 313 (2005) 245-249.

[31] C. J. Yang, X. Chen, H. Y. Chen, W. C. Zhuang, Y. C. Chai, J. C. Hao. J. Phys. Chem. B 110 (2006) 21735-21740.

[32] Y. R. Zhao, X. Chen, X. D. Wang. J. Phys. Chem. B 113 (2009) 2024-2030.